

# Acyclic and Cyclic Di- and Tri(4-oxophenyl-1,2-phenyleneethynylene)s: Their Synthesis and Ferromagnetic Spin Interaction

Hiroyuki Nishide,\* Masahiro Takahashi, Junichi Takashima, Yong-Jin Pu, and Eishun Tsuchida

Department of Polymer Chemistry, Waseda University, Tokyo 169-8555, Japan

Received March 31, 1999

A new set of  $\pi$ -conjugated and alternant but non-Kekulé-type di- and tri(1,2-phenyleneethynylene)s pendantly substituted with phenoxy radicals at the 4 positions (**1a**, **2a**, and **3a**) was synthesized. The synthesis of these acyclic and cyclic compounds was achieved through the head-to-tail coupling of 2-bromo(or -iodo)-4-[3',5'-di-*tert*-butyl-4'-trimethylsilyloxy(or -hydroxy)phenyl]-1-ethynylbenzenes. The di- and triphenoxy compounds (**1a**, and **2a** and **3a**) were triplet and quartet at the ground state, respectively, which was ascribed to a ferromagnetic coupling effect of the diphenyl ethynylene bridge for the pendant phenoxy radicals' spins. The cyclic  $\pi$ -conjugation in **3a** exhibited a stronger effect on the spin alignment.

## Introduction

Much effort has been continuously expended in synthesizing very high-spin and purely organic molecules that are expected to display molecular-based and unknown magnetism caused by intramolecular through-bond spin ordering.<sup>1,2</sup> A  $\pi$ -conjugated and alternant but non-Kekulé-type organic molecule bears plural radical centers, and some of its isomers are multiplet at the ground state. One of the ways to extend these non-Kekulé-type molecules to very high-spin molecules is to synthesize a  $\pi$ -conjugated linear polymer bearing pendant radical groups on every monomer unit, which are substituted on the polymer backbone to satisfy a  $\pi$ -conjugated and alternant but non-Kekulé-type structure. For example, we experimentally examined non-Kekulé-type stilbene diradicals and a triplet ground state of a meta-, para'-disubstituted isomer with relative stability;<sup>3</sup> we extended the triplet stilbene diradical to poly[4-(radical substituted)-1,2-phenylenevinylene]s, such as poly[4-(3',5'-di-*tert*-butyl-4'-oxyphenyl)-1,2-phenylenevinylene] (Chart 2), and reported a strong ferromagnetic interaction between the pendant radical's spins through its  $\pi$ -conjugated backbone, poly(1,2-phenylenevinylene) for example, and five spins alignment on average.<sup>4</sup> Such

pendant-type radical polymers have the following advantages as a high-spin molecule: (i) The spin coupling is not sensitive to spin defects. (ii) The spins are expected to interact also among their remote spins. (iii) A chemically stable radical species can be introduced to the  $\pi$ -conjugation as the pendant group. To increase such a high-spin alignment, research on the very high-spin molecules including the pendant-type ones has recently focused on a still larger molecule with a higher dimension, i.e., star-shaped, dendric, macrocyclic, and ladder homologues.<sup>2</sup>

On the other hand, novel graphitic carbon allotropes as a planar and two-dimensionally  $\pi$ -conjugated framework is an area of intense investigation.<sup>5</sup> A typical example is graphyne<sup>5e</sup> (Chart 3), and its subunits are acyclic and cyclic tri(1,2-phenyleneethynylene)s. While acyclic oligo- and poly(phenyleneethynylene)s with a 1,3-(meta)- or 1,4-(para)-substitution on the benzene ring have been well studied,<sup>6</sup> only Grubbs and Kratz reported the synthesis, structure, and  $\pi$ -conjugated property of acyclic oligo- and poly(1,2-(ortho)-phenyleneethynylene)s.<sup>7</sup> Cyclic tri(1,2-phenyleneethynylene), i.e., tribenzotrisedehydro[12]annulene, is well-known and characterized by a triangular and coplanar  $\pi$ -conjugation.<sup>5e,8</sup> The acyclic and cyclic 1,2-phenyleneethynylenes are expected to be one of the effective  $\pi$ -conjugated backbones to ferromagnetically connect the pendant radical's spins and to be the unit for extending the high-spin part to a (pseudo) two-

(1) For reviews on high-spin organic molecules, see: (a) Dougherty, D. A. *Acc. Chem. Res.* **1991**, *24*, 88. (b) Iwamura, H.; Koga, N. *Acc. Chem. Res.* **1993**, *26*, 346. (c) Rajca, A. *Chem. Rev.* **1994**, *94*, 871. (d) Nishide, H. *Adv. Mater.* **1995**, *7*, 937. (e) Lahti, P. M. *Magnetic Properties of Organic Materials*; Marcel Dekker: New York, 1998.

(2) For recent papers on very high-spin organic molecules, see: (a) Rajca, A.; Lu, K.; Rajca, S. *J. Am. Chem. Soc.* **1997**, *119*, 10355. (b) Rajca, A.; Wongsriratanakul, J.; Rajca, S. *J. Am. Chem. Soc.* **1997**, *119*, 11674. (c) Ruiz-Molina, D.; Veciana, J.; Palacio, F.; Rovira, C. *J. Org. Chem.* **1997**, *62*, 9009. (d) Rajca, A.; Wongsriratanakul, J.; Rajca, S.; Cerny, R. *Angew. Chem., Int. Ed. Engl.* **1998**, *37*, 1229. (e) Bushby, R.; Gooding, D. *J. Chem. Soc., Perkin Trans. 2* **1998**, 1069. (f) Nishide, H.; Miyasaka, M.; Tsuchida, E. *Angew. Chem., Int. Ed. Engl.* **1998**, *37*, 2400. (g) Nishide, H.; Miyasaka, M.; Tsuchida, E. *J. Org. Chem.* **1998**, *63*, 7399.

(3) Yoshioka, N.; Lahti, P. M.; Kaneko, T.; Kuzumaki, Y.; Tsuchida, E.; Nishide, H. *J. Org. Chem.* **1994**, *59*, 4272.

(4) (a) Kaneko, T.; Toriu, S.; Kuzumaki, Y.; Nishide, H.; Tsuchida, E. *Chem. Lett.* **1994**, 2135. (b) Nishide, H.; Kaneko, T.; Nii, T.; Katoh, K.; Tsuchida, E.; Yamaguchi, K. *J. Am. Chem. Soc.* **1995**, *117*, 548. (c) Nishide, H.; Kaneko, T.; Nii, T.; Katoh, K.; Tsuchida, E.; Lahti, P. M. *J. Am. Chem. Soc.* **1996**, *118*, 9695.

(5) (a) Diederich, F. *Nature* **1994**, *369*, 199. (b) Bunz, U. H. F.; Wiegmann-Kreiter, J. E. C. *Chem. Ber.* **1996**, *129*, 785. (c) Haley, M. M.; Brand, S. C.; Pak, J. J. *Angew. Chem., Int. Ed.* **1997**, *36*, 836. (d) Baughman, R. H.; Eckhardt, H.; Kertesz, M. *J. Chem. Phys.* **1987**, *87*, 6687. (e) Eickmeier, C.; Junga, H.; Matzger, A. J.; Scherhag, F.; Shim, M.; Vollhardt, K. P. C. *Angew. Chem., Int. Ed. Engl.* **1997**, *36*, 2103.

(6) (a) Weder, C.; Wrighton, M. S. *Macromolecules* **1996**, *29*, 5157. (b) Sanechika, K.; Yamamoto, T.; Yamamoto, A. *Bull. Chem. Soc. Jpn.* **1984**, *57*, 752. (c) Trumbo, D. L.; Marvel, C. S. *J. Polym. Sci., Polym. Chem. Ed.* **1986**, *24*, 2311.

(7) Grubbs, R. H.; Kratz, D. *Chem. Ber.* **1993**, *126*, 149.

(8) (a) Wolovsky, R.; Sondheimer, F.; Gattatt, P. J.; Calder, I. C. *J. Am. Chem. Soc.* **1965**, *87*, 5720. (b) Campbell, I. D.; Eglington, G.; Henderson, W.; Raphael, R. A. *Chem. Commun.* **1996**, 87. (c) Staab, H. A.; Graf, F. *Chem. Ber.* **1970**, *103*, 1107. (d) Kloster-Jensen, E.; Wirz, J. *Angew. Chem., Int. Ed. Engl.* **1973**, *12*, 671.

Chart 1

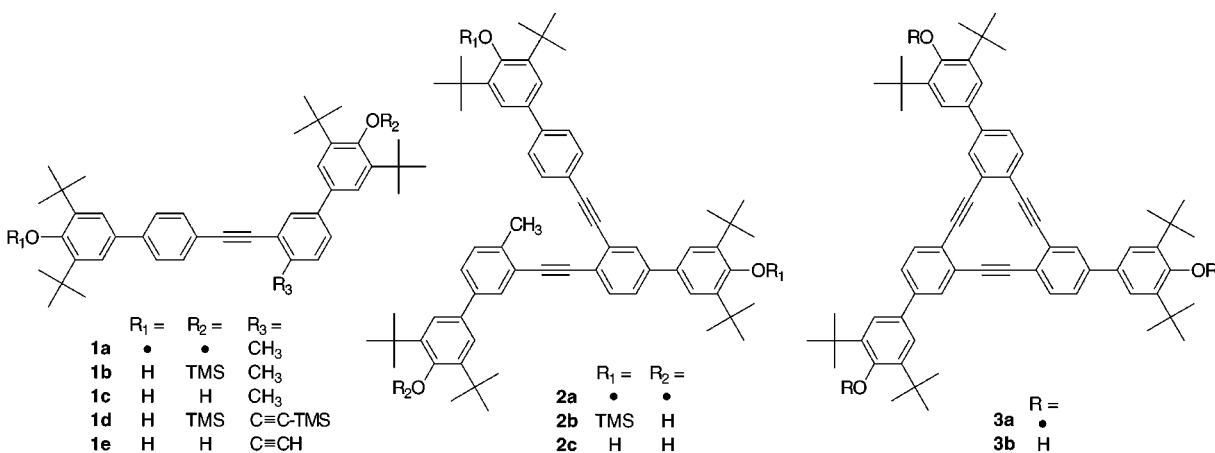


Chart 2

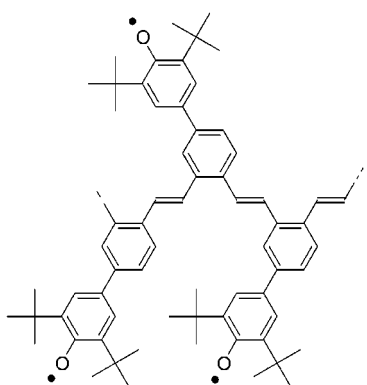
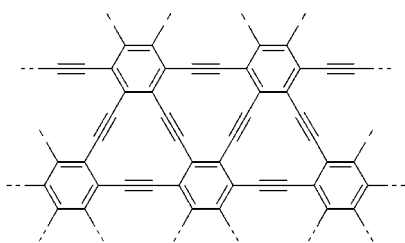


Chart 3



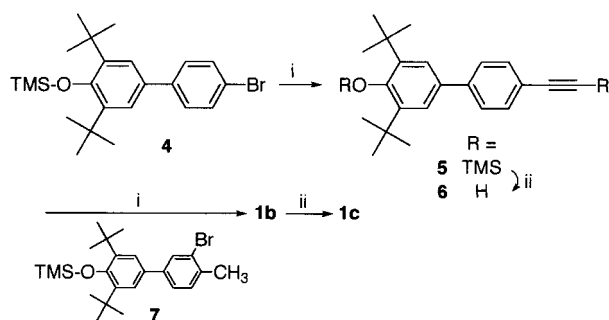
dimensional framework. However, to our knowledge, pendant-type radicals attached to an acyclic or cyclic oligo(1,2-phenyleneethynylene) have not been reported. In this paper, we have first synthesized acyclic and cyclic di- and tri(1,2-phenyleneethynylene)s pendants 4-substituted with 3',5'-di-*tert*-butyl-4'-oxyphenyl groups and examined their high-spin state.<sup>9</sup>

## Results and Discussion

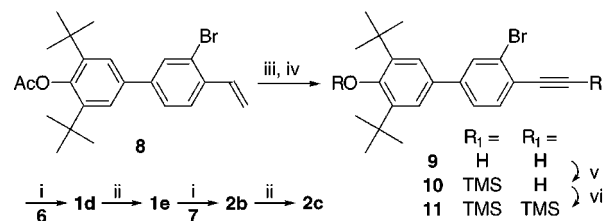
**Synthesis.** A restricted primary structure or complete head-to-tail linkage of the monomer unit is essential for a ferromagnetic high-spin state in the pendant-type oligoradical, which was established for the precursors of acyclic di- and tri(4-oxyphenyl-1,2-phenyleneethynylene)s, **1b** and **2b** (Chart 1), through the cross-coupling reactions in the presence of a palladium-triphenylphosphine catalyst and cuprous iodide.

3,4'-Bis[4'-(3'',5''-di-*tert*-butyl-4''-hydroxyphenyl)]diphenylethylenes, **1c** and **1e**, were prepared as shown in

Scheme 1



Scheme 2



Scheme 1. 4-(3',5'-Di-*tert*-butyl-4'-hydroxyphenyl)ethynylbenzene **6** was prepared via a cross-coupling reaction of 1-bromo-4-(3',5'-di-*tert*-butyl-4'-trimethylsilyloxyphenyl)benzene with trimethylethynylsilane and the following elimination of the protecting silyl (TMS: trimethylsilyl) groups. A cross-coupling of **6** with the 2-bromo-4-(3',5'-di-*tert*-butyl-4'-trimethylsilyloxyphenyl)toluene **7** (or **1e**) and subsequent elimination of the TMS group yielded **1c** (or **1e**).

The acyclic tri(4-hydroxyphenyl-1,2-phenyleneethynylene) **2c** was synthesized, as shown in Scheme 2. The vinyl group of 2-bromo-(3',5'-di-*tert*-butyl-4'-acetoxyphenyl)-styrene<sup>4b</sup> **8** was converted to the ethynyl group via the addition of bromine and the following elimination of hydrogen bromide. **9** was stepwisely protected with TMS groups to give **11**, which was cross-coupled with **6**. Elimination of the TMS groups yielded **1e**. The cross-coupling of **1e** with **7** and subsequent elimination of the TMS group gave **2c**.

To obtain the cyclic tri(4-hydroxyphenyl-1,2-phenyleneethynylene) or a dehydro[12]annulene symmetrically annelated with a phenol-bearing benzene **3b**, we tried the cross-coupling of the 2-bromo-4-ethynylbenzene derivatives **9** and **10**; however, **3b** was not formed. The bromo substituent in **11** was substituted with iodine,

(9) Our preliminary paper on the cyclic tri(1,2-phenyleneethynylene) 4-substituted with oxyphenyl groups: Pu, Y.-J.; Takahashi, M.; Tsuchida, E.; Nishide, H. *Chem. Lett.* **1999**, 161.

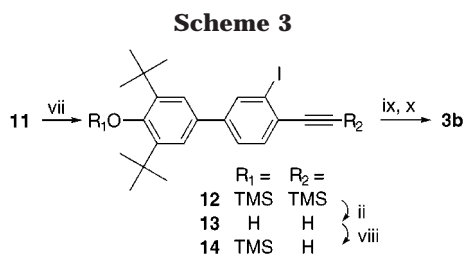


**Table 1. UV/vis Absorption and Fluorescence Maxima and Redox Potential of the Hydroxy Precursors**

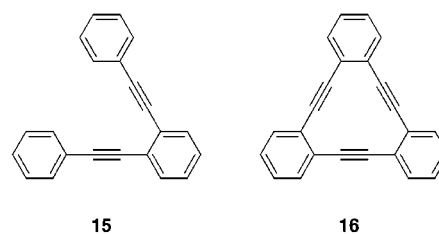
compd	UV abs <sup>a</sup> $\lambda_{\max}$ , nm (log $\epsilon_{\max}$ )	fluorescence <sup>b</sup> $\lambda_{\text{em}}$ , nm ( $\Phi$ )	redox potential <sup>c</sup> (V)
<b>1b</b>	312 (4.4)	361	0.01
<b>2b</b>	314 (4.5)	387	0.01
<b>15</b>	272 (4.7)		
<b>3b</b>	333 (5.1)	500 (0.12)	0.01
<b>16</b>	287 (5.4)	485 (0.07)	

<sup>a</sup> Chloroform solution. <sup>b</sup> Benzene solution,  $\lambda_{\max} = 420$  nm,  $\Phi$ : quantum yield normalized with 9,10-diphenylanthracene ( $\Phi = 0.84$ ). <sup>c</sup> Redox potential in the methylene dichloride solution of 6 equiv  $(\text{CH}_3)_4\text{NOH}$  and 0.1 M  $(\text{CH}_3)_4\text{NBF}_4$  as an alkali and electrolyte, respectively, vs Ag/AgCl (ref Fc/Fc<sup>+</sup> = 0.58 V).

using *n*-butyllithium, to improve the reactivity of the *o*-halogenoethynylbenzene. The hydroxy and ethynyl groups of **12** were deprotected to afford **13**. A selective protection of the hydroxy group of **13** yielded **14**. The cuprous acetylide derivative of **14** was condensed in pyridine to give the annulene derivative **3b**. **Structure**. The acyclic hydroxy precursors, **1c** and **2c**, were dissolved well in common solvents such as benzene, THF, and chloroform. On the other hand, the solvent solubility of the cyclic precursor **3b** was low, probably due to its large planar aromatic structure. FAB mass spectroscopy of **1c**, **2c**, and **3b** agreed with their calculated values. The fluorescence of these compounds was attributed to the diphenyl ethynylene moiety. <sup>13</sup>C and <sup>1</sup>H NMR peaks ascribed to the benzene rings and the ethynylene bridge of **1c**, **2c**, and **3b** supported both the phenyleneethynylene bonds and the head-to-tail linkage structure (for details, see the Experimental Section). The cyclic precursor **3b** gave 12 absorption peaks in the <sup>13</sup>C NMR, which indicates a  $C_3$  symmetrical structure of the cyclic **3**. In the <sup>1</sup>H NMR data, the signals for the nine protons on the annelated benzene ring of **3b** were slightly shifted upfield ( $\Delta\delta = 0.1\text{--}0.2$ ) relative to the corresponding monomeric and acyclic units, which correlates with the paramagnetic ring current of the cyclic annulene ring.

A preliminary tool to estimate the  $\pi$ -conjugation of the phenyleneethynylene backbone is the UV absorption and fluorescence spectroscopic data collected in Table 1. The absorption and fluorescence maxima of the phenyleneethynylene bathochromically shifted from the dimer to the acyclic and the cyclic trimer. These shifts reflect the increase in number of the phenyleneethynylene units. The maxima of **2b** and **3b** also bathochromically shifted in comparison with those of **15** and **16**, which are ascribed to the developed  $\pi$ -conjugation due to the three phenol groups. Electrochemical redox of the pendant but  $\pi$ -conjugated phenol with the phenyleneethynylene will give additional information on the backbone. The cyclic voltammograms of **1c**, **2c**, and **3b** exhibited completely reversible but simple redox waves ascribed to the phenolate/phenoxyl redox couple, in alkaline dichloromethane solution under a nitrogen atmosphere. This means that the phenoxyl radicals are chemically stable even in

**Chart 4**



solution at room temperature and that the radical generation is not accompanied by a subsequent chemical side reaction. The redox potentials of the phenolate/phenoxyl given in Table 1 are ca. 0.01 V for **1c**, **2c**, and **3b**. Differential pulse voltammetry was applied to the oxidation of these phenol derivatives; however, it gave only a unimodal current peak. These results indicate that the diphenylethynylene coupler is too long in the  $\pi$ -conjugation and/or steric distance to induce an effect on the redox reaction.

**ESR Spectra of the Phenoxyl Radicals.** The phenoxyl radicals, **1a**, **2a**, and **3a**, were obtained by heterogeneously treating the toluene solutions of **1c**, **2c**, and **3b** with aqueous alkaline  $\text{K}_3\text{Fe}(\text{CN})_6$  solution or with fresh  $\text{PbO}_2$  powder. The toluene solutions rapidly turned deep green: The appearance of a new absorption peak at ca. 640 nm suggests the formation of phenoxyl radicals. Although the oxidation of **1e** did not yield a stable radical probably due to a radical coupling reaction between the ethynyl groups of **1e**, the methyl-protected derivative **1c** formed a stable radical.

The ESR spectra of the monoradicals of **9**, **2c**, and **3b** [for the latter two; i.e., **2a** and **3a** with a very low spin concentration (spin concn = spin/monomeric phenol residue unit)] gave a hyperfine structure attributed to 5–6 protons of the phenoxyl ring and the phenyleneethynylene backbone (Figure 1), which was in contrast to the simple three-line hyperfine structure of 2,4,6-*tert*-butylphenoxyl or that attributed to an unpaired electron localized in the phenoxyl ring. The dashed line in Figure 1a shows a simulation of the hyperfine structure of the monomeric unit (the monoradical of **9**), which gave the four  $a_{\text{H}}$  values attributed to the five protons of the phenoxyl and phenylene rings and to the remote proton of the ethynyl group. The monoradical of the corresponding dimer **2c** gave a similar hyperfine structure in the ESR spectrum (Figure 1b). The ESR spectrum of the monoradical of **3b** showed a clearer hyperfine structure, which was assigned to the two protons of the phenoxyl ring and three protons of the annulene backbone (Figure 1c). These ESR results indicate an effectively delocalized spin distribution into the phenyleneethynylene backbone.

The ESR spectra of **1a**, **2a**, and **3a** showed sharp and unimodal signals with increasing spin concn; the spectra in the frozen toluene glass exhibited a  $\Delta M_s = \pm 2$  forbidden transition ascribed to a triplet species at  $g = 4$  (inset in Figure 2). The ESR signal in the  $\Delta M_s = \pm 2$  region was doubly integrated to give Curie plots (Figure 2). Although the signal intensities are proportional to the reciprocal of the temperature ( $1/T$ ) at higher temperature, the plots deviate upward from linearity in the lower temperature (<10 K) region, especially for **3a**. The upward deviation of the  $\Delta M_s = \pm 2$  transition means an enhancement of probability of the triplet and/or quartet

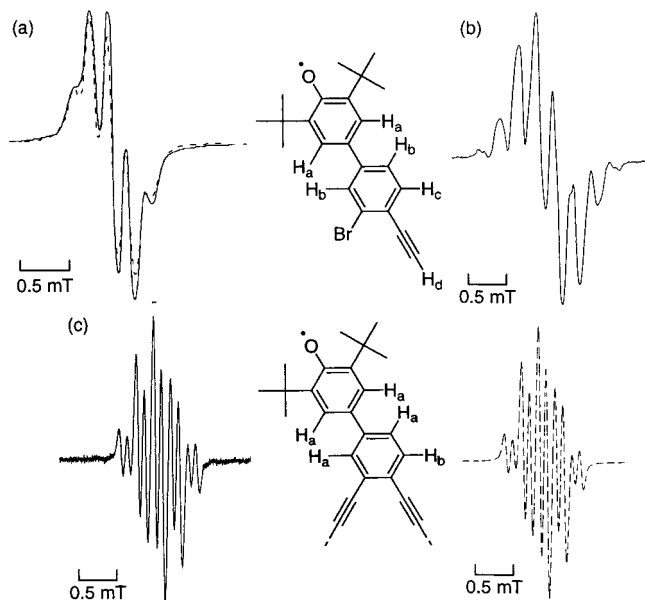


**Figure 1.** ESR spectra of (a) the radical of **9**, (b) the monoradical of **2c**, and (c) the monoradical of **3b** in toluene at room temperature. Precursor phenol concentration = 0.5 unit mM. (a) Monoradical of **9** with spin concentration = 0.9,  $g = 2.0044$ ; the dashed line for the simulation with  $a_{\text{Ha}} = 0.18$ ,  $a_{\text{Hb}} = 0.17$ ,  $a_{\text{Hc}} = 0.06$ , and  $a_{\text{Hd}} = 0.05$  mT. (b) Monoradical of **2c** with spin concentration = 0.025,  $g = 2.0042$ . (c) Monoradical of **3b** with spin concentration = 0.0001,  $g = 2.0043$ ; dashed line for the simulation with  $a_{\text{Ha}} = 0.18$ ,  $a_{\text{Hb}} = 0.08$  mT.

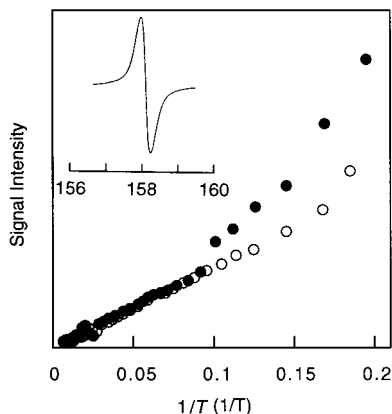


**Figure 2.** Curie plots for the peak in the  $\Delta M_s = \pm 2$  regions for the acyclic diphenoxyl **1a** (○) with spin concentration = 0.70 spin/unit and the cyclic triphenoxyl **3a** (●) with spin concentration = 0.70 spin/unit in toluene glass. Precursor phenol concentration = 30 unit mM. Inset:  $\Delta M_s = \pm 2$  spectrum for **1a**.

ground states in the low temperature and a ferromagnetic interaction between the phenoxy spins.

**Magnetic Properties.** The static magnetic susceptibility ( $\chi$ ) and magnetization ( $M$ ) of the acyclic diphenoxyl **1a** and triphenoxyl **2a** and the cyclic triphenoxyl **3a**, in frozen toluene or 2-methyltetrahydrofuran, were measured using a SQUID magnetometer. For example, normalized plots of magnetization ( $M/M_{\text{sat}}$ ) for **1a** were presented close to the Brillouin curve for  $S = 2/2$  at 2–10 K (inset of Figure 3), indicating a triplet ground state of the diradical **1a**.

The spin-exchange coupling constant of the intramolecular spin-alignment through the  $\pi$ -conjugated bond (positive for a ferromagnetic coupling) was estimated for

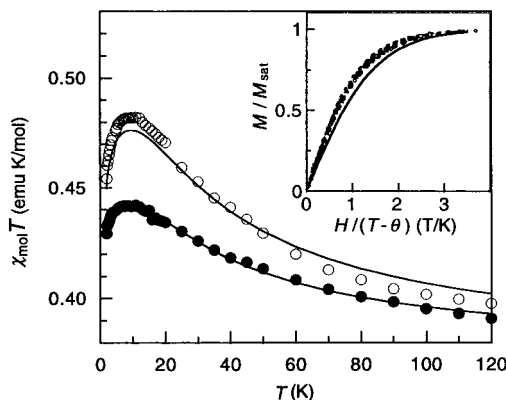


**Figure 3.**  $\chi_{\text{mol}}T$  vs  $T$  plots (○) of the diphenoxyl **1a** with spin concentration = 0.72 spin/unit and  $\chi_{\text{mol}}T$  vs  $T$  plots (●) of the triphenoxyl **2a** with spin concentration = 0.92 spin/unit in frozen 2-methyltetrahydrofuran. Solid lines are theoretical curves calculated using equations<sup>10</sup> for **1a** ( $2J = 31$  cm<sup>-1</sup>,  $\theta = -0.12$  K,  $x_1 = 0.43$ ,  $x_2 = 0.57$ ) and **2a** ( $2J = 31$  cm<sup>-1</sup>,  $\theta = -0.16$  K,  $x_1 = 0.16$ ,  $x_2 = 0.79$ ,  $x_3 = 0.05$ ), respectively. Inset: Normalized plots of magnetization ( $M/M_{\text{sat}}$ ) vs the ratio of magnetic field and temperature ( $H/(T - \theta)$ ) for the **1a** at  $T = 1.8$  (○), 2 (●), 2.5 (□), 3 (■) K. The theoretical curves correspond to the  $S = 1/2$  and  $2/2$  Brillouin functions.

the acyclic bi- and triradical **2a** and **3a** by curve fitting the  $\chi_{\text{mol}}T$  vs  $T$  data (Figure 3) to the equation derived from a linear three- or two-spin model based on the Heisenberg Hamiltonian.<sup>10</sup> The resulting parameters are summarized in the caption of Figure 3. The spin-exchange constant or stability of the triplet ground-state  $2J$  (or  $\Delta E_{T-S}$ ) values for **1a** and **2a** were estimated to be 31 and 32 cm<sup>-1</sup>, respectively. These values were smaller than those of *m,p'*-bis(3,5-di-*tert*-butyl-4-oxophenyl)stilbene ( $2J = 50$  cm<sup>-1</sup>).<sup>4b,c</sup> This result does not conflict with the prediction of  $\Delta E_{T-S}$  using semiempirical AM1 computation for the meta,para'-disubstituted diradicals based on stilbene (or toluene backbone) by Lahti et al.<sup>11</sup> They explained that the toluene backbone is not as effective as a ferromagnetic coupler because it lacks the alternativity of single-double bonds in the  $\pi$ -conjugation at the ethynylene triplet bond bridge.

The  $M/M_{\text{sat}}$  plots of **3a** with a spin concn = 0.81 spin/unit lie almost on the Brillouin curve for  $S = 3/2$  at 1.8–20 K, indicating a quartet ground state and a ferromagnetic spin alignment between the pendant phenoxy electrons through the cyclic  $\pi$ -conjugation tribenzotrisdehydro[12]annulene.

The  $J$  value was estimated by curve fitting<sup>12</sup> the  $\chi_{\text{mol}}T$  vs  $T$  data (inset of Figure 4) to the equation derived from a triangular three-spin model based on the Heisenberg Hamiltonian.<sup>11</sup>  $2J$  was evaluated to be 48 cm<sup>-1</sup>. This  $2J$

(10)  $\chi_{\text{mol}}T = N_A g^2 \mu_B^2 T \{ x_3 \{ 1 + \exp[-2J/(kT)] + 10 \exp[J/(kT)] \} / \{ 12 - \{ 1 + \exp[-12J/(kT)] + 2 \exp[J/(kT)] \} \} + x_2 \{ 3 + \exp[-2J/(kT)] \} + x_1 / 4 \} / [k(T - \theta)]$ , where  $2J$ ,  $\theta$ ,  $x_1$ ,  $x_2$ , and  $x_3$  are the effective magnetic moment, the spin exchange coupling constant, the Weiss constant for a weak intermolecular magnetic interaction, and the fraction of doublet ( $S = 1/2$ ), the triplet ( $S = 1$ ), and the quartet ( $S = 3/2$ ), respectively.  $x_3 = 0$  for a two-spin system. (a) Bleaney, B.; Bowers, K. D. *Proc. R. Soc. London* **1952**, *A214*, 451. (b) Vleck, J. H. V. *The Theory of Electric and Magnetic Susceptibilities*; Oxford University Press: London, 1932.

(11) (a) Lahti, P. M.; Ichimura, A. S. *J. Org. Chem.* **1991**, *56*, 3030. (b) Lahti, P. M.; Ichimura, A. S. *Mol. Cryst. Liq. Cryst.* **1989**, *176*, 125.

(12)  $\chi_{\text{mol}}T = N_A g^2 \mu_B^2 T \{ x_3 \{ 2 + 10 \exp[3J/(kT)] \} / \{ 12 \{ 2 + \exp[3J/(kT)] \} \} + x_2 \{ 3 + \exp[-2J/(kT)] \} + x_1 / 4 \} / [k(T - \theta)]$ . (a) Carlin, R. L. *Magnetochemistry*; Springer-Verlag: Berlin, 1986. (b) Fujita, J.; Tanaka, M.; Suemune, H.; Koga, N.; Matsuda, K.; Iwamura, H. *J. Am. Chem. Soc.* **1996**, *118*, 9347.

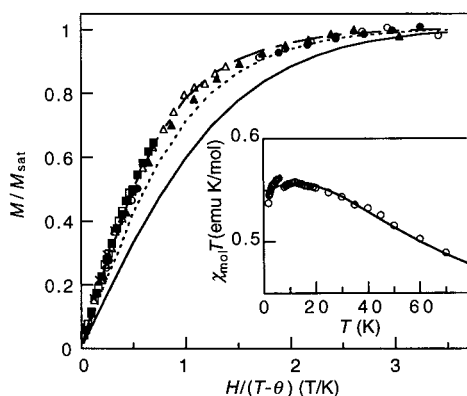


**Figure 4.**  $M/M_s$  vs  $H/(T - \theta)$  plots for the cyclic triphenoxyl **3a** with spin concentration = 0.81 spin/unit in frozen toluene at 1.8 (○), 2.0 (●), 2.25 (□), 5 (■), 10 (△), 15 (▲), 20 (×) K, and the theoretical Brillouin curves for  $S = 1/2$ ,  $2/2$ , and  $3/2$ . Inset:  $\chi_{\text{mol}}T$  vs  $T$  plots of the **3a**. Solid line is a theoretical curve calculated using the equation<sup>12</sup> for **3a** ( $2J = 48 \text{ cm}^{-1}$ ,  $\theta = -0.052 \text{ K}$ ,  $x_1 = 0.07$ ,  $x_2 = 0.40$ ,  $x_3 = 0.53$ ).

value of **3a** is larger than those estimated above for **1a** and **2a**. The strong exchange interaction is probably ascribed to the coplanarity of the annulene ring and more effective spin distribution of the pendant phenoxy radicals through the backbone conjugation of this annulene.

Because the tribenzotrisedehydro[12]annulene can be further modified into a two-dimensional extension, the pendant-type and cyclic triradical **3a** would become an effective quartet unit for the purpose of synthesizing a very high-spin polyradical.

## Experimental Section

**Cross-Coupling of the Acetylenic Compounds with the Aryl Bromides (Procedure i in Schemes 1–3).** A THF solution of an aryl bromide (1 equiv) and an acetylenic compound (1 equiv) were added to a THF solution of tetrakis-(triphenylphosphine)palladium(0) (0.05 equiv), cuprous iodide (0.02 equiv), and dry triethylamine (15 equiv). In the coupling reaction of trimethylsilylacetylene, it was added to the reaction mixture of an aryl bromide and the catalyst with a syringe. The reaction mixture was stirred under nitrogen at 70 °C for 17 h and monitored using thin-layer chromatography (TLC). The mixture was extracted with ether, and the extract was washed with water, dried over anhydrous sodium sulfate, and evaporated to give a crude product.

**Deprotection of the Trimethylsilyl Group (Procedure ii in Schemes 1–3).** A methanol/THF (or methylene dichloride) (1/1) solution of the TMS derivative was stirred after the addition of aqueous sodium hydroxide (5 equiv) under nitrogen atmosphere at 50 °C. The reaction was monitored by TLC and took 3–6 h. The mixture was diluted with water, neutralized with aqueous ammonium chloride, and extracted with ether. The extract was washed with water, dried over anhydrous sodium sulfate, and evaporated to afford the crude acetylenic derivative.

**3-(3',5'-Di-*tert*-butyl-4'-hydroxyphenyl)-6-methyl-4'-[3',5'-di-*tert*-butyl-4'-(trimethylsilyloxy)phenyl]tolane (1c).** **1b** (0.9 g, 1.34 mmol) was deprotected according to procedure ii. The crude product was purified using silica gel with a chloroform/hexane (1/5) eluent ( $R_f$  0.18) to afford **1c** (0.70 g) as a white powder: yield 88%;  $^1\text{H NMR}$  ( $\text{CDCl}_3$ , 500 MHz; ppm)  $\delta$  7.22–7.69 (m, 11H, Ar), 5.30 (s, 1H, OH), 5.25 (s, 1H, OH), 2.55 (s, 3H, Ar-CH<sub>3</sub>), 1.50 (s, 36H, *tert*-butyl);  $^{13}\text{C NMR}$  ( $\text{CDCl}_3$ , 125 MHz; ppm)  $\delta$  153.9, 153.5, 142.0, 139.7, 138.2, 136.3, 136.2, 131.9, 131.7, 130.1, 129.8, 128.3, 126.9, 126.8, 123.9, 123.8, 123.4, 121.5, 93.4, 88.9, 34.5, 30.4, 20.4; IR (KBr pellet,  $\text{cm}^{-1}$ ) 3634 ( $\nu_{\text{O-H}}$ ), 2209 ( $\nu_{\text{C=C}}$ ); MS (EI)  $m/e$  600, calcd

for  $\text{C}_{43}\text{H}_{52}\text{O}_2$  600.9. Anal. Calcd for  $\text{C}_{43}\text{H}_{52}\text{O}_2$ : C, 86.0; H, 8.7; O, 5.3. Found: C, 85.9; H, 8.5.

**2-Bromo-4-(3',5'-di-*tert*-butyl-4'-hydroxyphenyl)ethynylbenzene (9).** 2-Bromo-4-(3',5'-di-*tert*-butyl-4'-acetoxyphenyl)styrene **8** was prepared according to our previous paper.<sup>4b,c</sup> A chloroform solution (16 mL) of bromine (3.0 g, 19 mmol) was slowly added into a chloroform solution (8 mL) of **8** (8.0 g, 19 mmol) at 0 °C. After being stirred for 5 min at room temperature, the mixture was washed with 5% aqueous sodium sulfite and extracted with chloroform. The extract was washed with water, dried over anhydrous sodium sulfate, and evaporated to afford 11.0 g of 2-bromo-4-(3',5'-di-*tert*-butyl-4'-hydroxyphenyl)-1-(1',2'-dibromoethyl)benzene as a white powder, which was used in the following reaction without any purification. A DMSO solution (250 mL) of the dibromide derivative (10 g, 17 mmol) was treated with 70% aqueous sodium hydroxide for 3 h at 50 °C. The mixture was neutralized with 10% aqueous ammonium chloride and extracted with ether. The extract was dried and evaporated. The crude product was purified using a silica gel column with a chloroform/hexane (1/5) eluent. Recrystallization from ethanol gave **9** (2.6 g) as colorless crystals: yield 50%; mp 141 °C;  $^1\text{H NMR}$  ( $\text{CDCl}_3$ , 270 MHz; ppm)  $\delta$  7.75 (d, 1H, Ar), 7.53–7.56 (m, 2H, Ar), 7.45 (d, 2H, Ar), 7.42 (d, 1H, Ar), 5.35 (s, 1H, OH), 3.39 (s, 1H, ≡C-H), 1.48 (s, 18H, *tert*-butyl);  $^{13}\text{C NMR}$  ( $\text{CDCl}_3$ , 68 MHz; ppm)  $\delta$  154.34, 144.26, 136.53, 134.14, 130.57, 130.14, 125.80, 125.50, 123.92, 121.85, 82.12, 81.76, 34.49, 30.28; IR (KBr pellet,  $\text{cm}^{-1}$ ) 3615 ( $\nu_{\text{O-H}}$ ), 3310 ( $\nu_{\text{C-H}}$ ), 2114 ( $\nu_{\text{C=C}}$ ); MS (EI)  $m/e$  385 ( $\text{M}^+$ ), 387 ( $\text{M}^+ + 2$ ) calcd for  $\text{C}_{22}\text{H}_{25}\text{OBr}$  385.34. Anal. Calcd for  $\text{C}_{22}\text{H}_{25}\text{OBr}$ : C, 68.6; H, 6.5; Br, 20.7; O, 4.2. Found: C, 68.5; H, 6.2; Br, 20.4.

**2,4'-Bis(3'',5''-di-*tert*-butyl-4''-hydroxyphenyl)-2'-[4''-(3''',5'''-di-*tert*-butyl-4'-hydroxyphenyl)phenyl]-5-methyltolane (2c).** **1e** (1.7 g, 2.8 mmol) and **7** (1.3 g, 2.8 mmol) were reacted according to procedure i and purified using silica gel column with a chloroform/hexane (1/3) eluent ( $R_f$  0.31) to afford **2b** (0.40 g) as a yellow powder, yield 15%. **2b** (0.40 g, 0.41 mmol) was deprotected according to procedure ii and purified using a silica gel column with a chloroform/hexane (1/3) eluent ( $R_f$  0.26) to afford **2c** (0.33 g): yield 88%;  $^1\text{H NMR}$  ( $\text{CDCl}_3$ , 500 MHz; ppm)  $\delta$  7.78–7.22 (m, 16H, Ar), 5.33 (s, 1H, OH), 5.29 (s, 1H, OH), 5.23 (s, 1H, OH), 2.58 (s, 3H, Ar-CH<sub>3</sub>), 1.49 (s, 54H, *tert*-butyl);  $^{13}\text{C NMR}$  ( $\text{CDCl}_3$ , 125 MHz; ppm)  $\delta$  154.1, 153.9, 153.5, 142.1, 141.8, 139.7, 138.5, 136.4, 136.3, 136.2, 132.4, 132.1, 131.7, 131.6, 131.0, 130.3, 130.2, 129.8, 128.3, 127.1, 126.7, 126.5, 126.2, 125.9, 123.9, 123.8, 123.7, 123.5, 93.4, 92.9, 92.2, 89.1, 34.5, 30.4, 20.6; IR (KBr pellet,  $\text{cm}^{-1}$ ) 3636 ( $\nu_{\text{O-H}}$ ), 2211 ( $\nu_{\text{C=C}}$ ), 2106 ( $\nu_{\text{C=C}}$ ); MS (FAB)  $m/e$  904.5 calcd for  $\text{C}_{65}\text{H}_{76}\text{O}_3$  905.3. Anal. Calcd for  $\text{C}_{65}\text{H}_{76}\text{O}_3$ : C, 86.2; H, 8.5; O, 5.3. Found: C, 86.0; H, 8.2.

**4-[3',5'-Di-*tert*-butyl-4'-(trimethylsilyloxy)phenyl]-2-iodo-[(trimethylsilyl)ethynyl]benzene (12).** *n*-Butyllithium in hexane (1.6 M, 4.0 mL) was slowly added to a THF solution (52 mL) of **11** (3.2 g, 6.0 mmol) at 80 °C. After the mixture was stirred for 15 min, a THF solution (5.5 mL) of iodine (3.1 g, 12 mmol) was added to the mixture. The mixture was stirred at room temperature for 1 h, washed with a saturated aqueous sodium sulfite, extracted with ether, and washed with water. The crude product was purified using silica gel column with a hexane eluent ( $R_f$  0.21). Recrystallization from ethanol afforded **12** (2.24 g) as colorless crystals: yield 64.4%;  $^1\text{H NMR}$  ( $\text{CDCl}_3$ , 500 MHz; ppm)  $\delta$  8.01 (q, 1H, Ar), 7.47 (d,  $J = 1.0 \text{ Hz}$ , 2H, Ar), 7.41 (s, 2H, Ar), 1.45 (s, 18H, *tert*-butyl), 0.43 (s, 9H, TMS), 0.29 (s, 9H, TMS);  $^{13}\text{C NMR}$  ( $\text{CDCl}_3$ , 125 MHz; ppm)  $\delta$  153.7, 143.3, 141.4, 136.8, 132.7, 130.5, 127.4, 126.1, 124.5, 106.7, 101.7, 98.8, 35.3, 31.2, 3.9, -0.1; IR (KBr pellet,  $\text{cm}^{-1}$ ) 2160 ( $\nu_{\text{C=C}}$ ); MS (EI)  $m/e$  576 calcd for  $\text{C}_{28}\text{H}_{41}\text{OSi}_2$  576.1.

**2,8,14-Trisoxypheyltribenzotrisedehydro[12]-annulene (3b).** A ethanol solution (20 mL) of **14** (0.90 g, 2.1 mmol) was added to a aqueous ammonium hydroxide solution (55 mL) of cuprous chloride (0.47 g, 4.7 mmol). The mixture was stirred at room temperature for 2.5 h to give a suspension of a yellow precipitation and a blue solution. The precipitation was collected, washed with successive water and ethanol, and dried to afford a copper(I) acetylide derivative (0.74 g, yield

71%), which was used in the next procedure without any purification. The cuprous acetylide derivative (0.16 g, 0.31 mmol) was dissolved in pyridine (6.0 mL), and the solution was refluxed for 10 h to afford a crude product as a yellow powder. The crude product was purified using silica gel column with a chloroform/hexane (3/5) eluent to give **3b** (0.030 g) as a yellow solid: yield 32%;  $^1\text{H NMR}$  ( $\text{CDCl}_3$ , 500 MHz; ppm)  $\delta$  7.52 (d,  $J = 1.8$  Hz, 3H, Ar), 7.43 (d,  $J = 8.3$  Hz, 3H, Ar), 7.38 (s, 6H, Ar), 7.35 (dd,  $J = 1.8, 8.3$  Hz, 3H, Ad), 5.32 (s, 3H, OH), 1.49 (s, 54H, *tert*-butyl);  $^{13}\text{C NMR}$  ( $\text{CDCl}_3$ , 125 MHz; ppm) 154.2, 142.5, 136.5, 132.5, 130.8, 130.2, 127.3, 126.9, 124.4, 123.8, 93.5, 93.1, 34.6, 30.5; IR (KBr pellet,  $\text{cm}^{-1}$ ) 3640 ( $\nu_{\text{O-H}}$ ), 2957 ( $\nu_{\text{C-H}}$ ); MS (FAB) *m/e* 913.6 ( $\text{M}^+$ ) calcd for  $\text{C}_{66}\text{H}_{72}\text{O}_3$  913.3. Anal. Calcd for  $\text{C}_{66}\text{H}_{72}\text{O}_3$ : C, 86.8; H, 8.0; O, 5.3. Found: C, 86.6; H, 7.9.

**Oxidation.** Aqueous solutions of sodium hydroxide and potassium ferricyanide (10 and 20 equiv to the phenol group, respectively) were added successively to a toluene or 2-methyltetrahydrofuran solution (1–20 mM) of the hydroxy precursor (**9**, **1c**, **2c**, or **3b**) with vigorous stirring at room temperature in a glovebox. The mixture was turned deeply green after 5 min. After the mixture was stirred for 30 min, the organic layer was separated, washed with water, and dried over anhydrous sodium sulfate to give the radical solution.

**ESR and SQUID Measurements.** ESR spectra were taken on a JEOL TE-200 ESR spectrometer with a 100 kHz field modulation. The spin concentration of each sample was determined both by careful integration of the ESR signal standardized with that of 2,2,6,6-tetramethyl-1-piperidinyloxy solution and by analyzing the saturated magnetization at the SQUID measurement.

The 2-methyltetrahydrofuran or toluene solutions of radicals were immediately transferred to a diamagnetic capsule after the oxidation. Magnetization and static magnetic susceptibility were measured with a Quantum Design MPMS-7 SQUID

magnetometer. The magnetization was measured from 0 to 7 T at 1.8, 2, 2.25, 2.5, 3, 5, 10, 15, and 20 K. The static magnetic susceptibility was measured from 1.8 to 200 K at a field of 0.5 T.

**Other Spectroscopic Measurements.** The  $^1\text{H}$  and  $^{13}\text{C}$  NMR, MS, FAB-MS, UV/vis, IR, and fluorescence spectra were measured using a JEOL Lambda 500 or a JNM-EX270, a Shimadzu GCMS-QP5050, a JMS-SX-102A, a JASCO V-500, a JASCO FT/IR-410, a Hitachi F-4500 spectrometer, respectively.

**Acknowledgment.** This work was partially supported by a Grant-in-Aid for Scientific Research (Nos. 09305060 and 277/08246101) from the Ministry of Education, Science and Culture, Japan, and by the NEDO Project on Technology for Novel High-Functional Materials.

**Supporting Information Available:** Syntheses and characterizations of 4-[3',5'-di-*tert*-butyl-4'-(trimethylsilyloxy)phenyl](trimethylsilyl)ethynyl benzene (**5**), 4-(3',5'-di-*tert*-butyl-4'-hydroxyphenyl)ethynylbenzene (**6**), 3-(3',5'-di-*tert*-butyl-4'-hydroxyphenyl)-6-methyl-4'-[3',5'-di-*tert*-butyl-4'-(trimethylsilyloxy)phenyl]-tolane (**1b**), 2-bromo-4-[3',5'-di-*tert*-butyl-4'-(trimethylsilyloxy)phenyl]ethynylbenzene (**10**), 1-[2-bromo-4-[3',5'-di-*tert*-butyl-4'-(trimethylsilyloxy)phenyl]phenyl]-2-(trimethylsilyl)acetylene (**11**), 5-(3'',5''-di-*tert*-butyl-4''-hydroxyphenyl)-4-[3'',5''-di-*tert*-butyl-4''-(trimethylsilyloxy)phenyl]-2-(trimethylsilyl)ethynyl toluene (**1d**), 5,4'-bis(3,5-di-*tert*-butyl-4-hydroxyphenyl)-2-ethynyltolane (**1e**), and 4-[3',5'-di-*tert*-butyl-4'-(trimethylsilyloxy)phenyl]-2-iodo-ethynylbenzene (**14**). This material is available free of charge via the Internet at <http://pubs.acs.org>.

JO990575I